Computer Methods and Programs in Biomedicine (2004) **74**, 95–108

ELSEVIER

Computer Methods and Programs in Biomedicine

www.intl.elsevierhealth.com/journals/cmpb

Automatic arrhythmia detection based on time and time–frequency analysis of heart rate variability

Markos G. Tsipouras, Dimitrios I. Fotiadis*

Unit of Medical Technology and Intelligent Information Systems, Department of Computer Science, University of Ioannina, GR 45110, Ioannina, Greece

Received 2 August 2002; received in revised form 27 January 2003; accepted 11 February 2003

KEYWORDS
Arrhythmia detection;
Heart rate variability;
Time–frequency analysis

Summary We have developed an automatic arrhythmia detection system, which is based on heart rate features only. Initially, the RR interval duration signal is extracted from ECG recordings and segmented into small intervals. The analysis is based on both time and time–frequency ($t-f$) features. Time domain measurements are extracted and several combinations between the obtained features are used for the training of a set of neural networks. Short time Fourier transform and several time – frequency distributions (TFD) are used in the $t-f$ analysis. The features obtained are used for the training of a set of neural networks, one for each distribution. The proposed approach is tested using the MIT-BIH arrhythmia database and satisfactory results are obtained for both sensitivity and specificity (87.5 and 89.5%, respectively, for time domain analysis and 90 and 93%, respectively, for $t-f$ domain analysis).

1. Introduction

Arrhythmia is a collective term for any cardiac rhythm that deviates from normal sinus rhythm. Arrhythmia may be due to a disturbance in impulse formation or conduction, or both, but it is not always an irregular heart activity [1]. Respiratory sinus arrhythmia is a natural periodic variation in RR-intervals, corresponding to respiratory activity. Impulse formation may be sinus or ectopic, the rhythm regular or irregular and the heart rate fast, normal or slow [2,3]. Therefore, the detection of abnormal cardiac rhythms and automatic discrimination from the normal heart activity became an important task for clinical reasons. Most of the studies address the detection and identification of life threatening arrhythmias and specifically ventricular and atrial fibrillation and ventricular tachycardia. Various detection algorithms have been proposed, such as the sequential hypothesis testing [4], the multiway sequential hypothesis testing [5], the threshold-crossing intervals [6], the auto-correlation function [6], the VF-filter [6] and algorithms based on neural-networks [7–9]. Time–frequency ($t-f$) analysis [10] and wavelet analysis [11,12] have also been used. Recent approaches utilize complexity measure [13] and multifractal analysis combined with a fuzzy Kohonen neural network [14].

Heart rate variability (HRV) refers to the beat-to-beat heart rate alterations. HRV believed to be a good marker of the individual's health condition and heart diseases [15]. Therefore, HRV

*Corresponding author. Tel.: +30-6510-98803; fax: +30-6510-97099.
E-mail addresses: markos@cs.uoi.gr (M.G. Tsipouras), fotiadis@cs.uoi.gr (D.I. Fotiadis).

0169-2607/$ – see front matter © 2003 Elsevier Ireland Ltd. All rights reserved.
doi:10.1016/S0169-2607(03)00079-8

analysis became a critical tool in cardiology for the diagnosis of heart diseases. Time domain analysis of RR-intervals includes calculation of several common statistical indices [16,17] and graphical representation of the RR-interval duration signal [18,19]. Frequency analysis provides the power spectrum density (PSD) of the RR-interval duration signal using Fourier transform and autoregressive techniques [20–25]. $t-f$ analysis is based on the use of short time Fourier transform (STFT), time–frequency distributions (TFDs) and wavelet analysis [10–12] of the RR-interval duration signal. Other approaches for the HRV analysis include methods from nonlinear mathematics and chaos theory, such as fractal [26,27] and approximate entropy [27] analysis.

More specifically in the $t-f$ analysis Wigner-Ville (WV) distribution [28,29] and improved forms of WV, such as pseudo Wigner-Ville (PWV) [30–33] and smoothed pseudo Wigner-Ville (SPWV) [34–36], discrete Fourier transform and selective discrete Fourier transform [37–40], cone shaped kernel distribution [10], Choi-Williams distribution [41] and other exponential distributions [42] have been used.

In this paper we explore time and $t-f$ analysis of the RR-interval duration signal in order to detect arrhythmic segments in ECGs [43]. Selected features from the time domain and $t-f$ analysis are extracted. Several combinations of those features are used for training a set of neural networks. The decision is finally obtained using decision rules.

2. Materials and methods

Our analysis is carried out in four stages. First a preprocessing procedure is used to extract the tachograms from the ECGs. The tachograms are segmented into small segments. Each segment contains 32 RR-intervals. In the second stage time domain or $t-f$ methods are applied to extract the corresponding features. In the third stage the extracted features are used for training a set of neural networks. In the forth stage detection of arrhythmic segments is carried out using decision rules which are fed with the outputs of the neural networks.

2.1. Preprocessing

Preprocessing is carried out in two steps. In the first step we extract the tachograms from the ECG recordings. The dataset used in our study is the MIT-BIH arrhythmia database [44,45]. This database consists of 48 ECG recordings. The length of each recording is 30 min, which results to a

Table 1 Beat annotations of the MIT-BIH arrhythmia database

Annotation symbol	Meaning	Classification in our case
N	Normal beat	Normal
L[a]	Left bundle branch block beat	Normal
R[a]	Right bundle branch block beat	Normal
A	Atrial premature beat	Arrhythmic
a	Aberrated atrial premature beat	Arrhythmic
J	Nodal (junctional) premature beat	Arrhythmic
S	Supraventricular premature beat	Arrhythmic
V	Premature ventricular contraction	Arrhythmic
F	Fusion of ventricular and normal beat	Arrhythmic
[	Start of ventricular flutter/fibrillation	Arrhythmic
!	Ventricular flutter wave	Arrhythmic
]	End of ventricular flutter/fibrillation	Arrhythmic
e	Atrial escape beat	Arrhythmic
j	Nodal (junctional) escape beat	Arrhythmic
n	Supraventricular escape beat	Arrhythmic
E	Ventricular escape beat	Arrhythmic
P[b]	Paced beat	Normal
f[b]	Fusion of paced and normal beat	Normal
p	Non-conducted P-wave (blocked APB)	Normal
Q	Unclassifiable beat	Normal
|	Isolated QRS-like artifact	Normal

[a] L and R annotated beats are classified as ''Normal'' because they cannot be detected as arrhythmic using only heart rate and HRV.
[b] Beats with annotations P and f are considered as normal because pace is not in the interest of this study.

total of 24 h of recordings with 112 568 RR-intervals. All RR-intervals are used except for those close to the start or end of each recording, which are excluded during segmentation. Each beat in the database is annotated with a character annotation (Table 1). The RDNN software, which accompanies the MIT-BIH database, is used for QRS detection. Then the RR-interval duration signal (tachogram) can be obtained.

In the second step the tachograms are cut into small segments of 32 RR-intervals each, and each segment is characterized as normal or arrhythmic using the MIT-BIH beat annotation. This results to 3456 segments. For each RR-interval the characterization of the second beat is used for its characterization. The characterization of the MIT-BIH arrhythmia database beats as ''normal'' or ''arrhythmic'' is shown in Table 1. A 32 RR-interval segment is characterized as ''normal'' if it contains more than 30 ''normal'' RR-intervals otherwise is characterized as ''arrhythmic''.

2.2. Time domain analysis

We apply time domain analysis on the segmented dataset. Time domain analysis results in indices and markers obtained from the tachogram, such as mean and standard deviation of RR-intervals, mean and standard deviation of differences between adjacent RR-intervals, difference between the longer and the shorter RR-interval and others. The standard deviation of all normal-to-normal RR-intervals (SDRR) is the simplest feature that can be extracted from the tachogram. The root mean square of successive differences of all normal-to-normal RR-intervals (r_MSSD) and the standard deviation of successive differences of all normal-to-normal RR-intervals (SDSD) are also widely used indices. The percentage of intervals presenting time duration difference between adjacent normal-to-normal RR-intervals greater than 50 ms (pNN50) is another HRV characteristic. In many studies this percentage is used with different time threshold, such as 5 ms (pNN5) or 10 ms (pNN10) [16,17].

We use all possible combinations among the above mentioned time analysis features (each combination contains one, two, three, four, five or six features) to create the pattern set for the classification stage. This leads to a total of 63 feature combinations, which are shown in Table 2, with 3426 patterns each. In the third stage (classification stage) we train a feed-forward back-propagation neural network, for each feature combination. We use 1426 patterns randomly chosen from the total of 3426 patterns as training set. Several neural network architectures have been tested and we have chosen the one that performs better: N inputs (number of features used in the specific combination), one hidden layer with 20 neurons and one output, being a real number between 0 and 1. The final ''normal'' or ''arrhythmic'' classification is made with 0.5 threshold on the networks' output. The training of the neural network ends when the square error is less than 0.01 or the training epochs are more than 2000. Finally, we result in a set with 63 neural networks (one for each combination). The outputs of the neural networks are fed into a set of decision rules as it is described below (forth stage).

2.3. Time–frequency analysis

STFT and various TFDs are used for the $t-f$ analysis of the segmented dataset. For STFT, the signal $x(u)$ is pre-windowed around a time instant t, and the Fourier Transform if calculated for each time

Table 2 Combinations of time domain features

	Feature combination	Features
1	1	SDNN
2	2	r_MSSD
3	12	SDNN, r_MSSD
4	3	SDSD
5	13	SDNN, SDSD
6	23	SDNN, r_MSSD
7	123	SDNN, r_MSSD, SDSD
8	4	pNN5
...	...	...
60	3456	SDSD, pNN5, pNN10, pNN50
61	13456	SDNN, SDSD, pNN5, pNN10, pNN50
62	23456	r_MSSD, SDSD, pNN5, pNN10, pNN50
63	123456	SDNN, r_MSSD, SDSD, pNN5, pNN10, pNN50

instant t.

$$\mathrm{STFT}(t,f)=\int_{-\infty}^{+\infty}x(\tau)h(\tau-t)e^{-if\tau}d\tau \quad (1)$$

where $h(t)$ is a short time window, localized around $t=0$ and $f=0$. STFT suffers of trade-off between its window length and its frequency resolution. The TFDs used in our study belong to the Cohen's class of distributions [46] and are given by the following formula:

$$\rho(t,f)=\int\int\int e^{i2\pi\upsilon(u-t)}g(\upsilon,\tau)\,x^*\left(u-\frac{1}{2}\tau\right)x\left(u+\frac{1}{2}\tau\right)e^{-i2\pi f\tau}d\upsilon du d\tau \quad (2)$$

where $x^*(t)$ is the complex conjugate of the signal and $g(\upsilon,\tau)$ is an arbitrary function called kernel. The kernel is different for each TFD. Table 3 shows selected TFDs, which are used in our study and the corresponding kernels [46–55].

For each 32 RR-interval segment STFT and all TFDs are applied (totally 19 methods) and the PSD is computed (Fig. 1). For STFT a Hamming nine-point length window is used. All TFDs, except Margenau-Hill, Page, Rihaczek and Wigner-Ville, use frequency and/or time smoothing windows, which were set as Hamming nine-point length windows. For the computation of the STFT and the TFDs for each segment we use the previous and the next segment to avoid problems in the margins of the segment. The PSD is computed and the amplitude is normalized in [−1,1] interval. This represents the fractional energy of the signal in time t and frequency f (Fig. 1a). We obtain horizontal slices from the PSD for amplitude = 0.0, 0.2, 0.4, 0.6, 0.8 and 1.0, which contain the corresponding PSD trace (Fig. 1b). The areas between adjacent slide traces are calculated (Fig. 1c and d). These areas are the $t-f$ features. Six features for each TFD are computed and they are used for the training of the neural networks (Fig. 2).

Table 3 TFDs

	Distribution	Kernel ($g(\upsilon,\tau)$)	
1	Born-Jordan	$\frac{\sin(\pi\upsilon\tau)}{\pi\upsilon\tau}$	
2	Butterworth	$\frac{1}{1+\left(\frac{\upsilon}{\upsilon_1}\right)^{2N}\left(\frac{\tau}{\tau_1}\right)^{2M}}$	$N,M,\upsilon_1,\tau_1>0$
3	Choi-Williams	$e^{-(\pi\upsilon\tau)^2/2\sigma^2}$	σ: scaling factor
4	Generalized rectangular	$\frac{\sin\left(\frac{2\pi\sigma\upsilon}{\lvert\tau\rvert^{\alpha}}\right)}{\pi\upsilon}$	σ: scaling factor; a: dissymmetry ratio
5	Margenau-Hill	$\mathrm{Cos}(\pi\upsilon\tau)$	
6	Pseudo Margenau-Hill	$h(\tau)\cos(\pi\upsilon\tau)$	$h(\tau)$: window function
7	Margenau-Hill-spectrogram	$h(\tau)\cos(\pi\upsilon\tau)A_x^*(\upsilon,\tau)$,	$A_x(\upsilon,\tau)$: ambiguity function
8	Page	$e^{j\pi\upsilon\lvert\tau\rvert}$	
9	Pseudo page	$h(\tau)e^{j\pi\upsilon\lvert\tau\rvert}$	$h(\tau)$: window function
10	Wigner-Ville	1	
11	PWV	$h(\tau)$	$h(\tau)$: window function
12	Smoothed PWV	$G(\upsilon)h(\tau)$	$h(\tau)$: window function
13	Rihaczek	$e^{j\pi\upsilon\tau}$	
14	Reduced interference (Bessel window)	$\int_{-\infty}^{+\infty}h(t)e^{-j2\pi\upsilon\tau t}dt$	$h(t)$: Bessel window
15	Reduced interference (Hanning window)	$\int_{-\infty}^{+\infty}h(t)e^{-j2\pi\upsilon\tau t}dt$	$h(t)$: Hanning window
16	Reduced interference (Binomial window)	$\int_{-\infty}^{+\infty}h(t)e^{-j2\pi\upsilon\tau t}dt$	$h(t)$: binomial window
17	Reduced interference (Triangular window)	$\int_{-\infty}^{+\infty}h(t)e^{-j2\pi\upsilon\tau t}dt$	$h(t)$: triangular window
18	Zhao-Atlas-Marks	$h(\tau)\frac{\sin(\pi\upsilon\tau)}{\pi\upsilon\tau}$	$h(\tau)$: window function

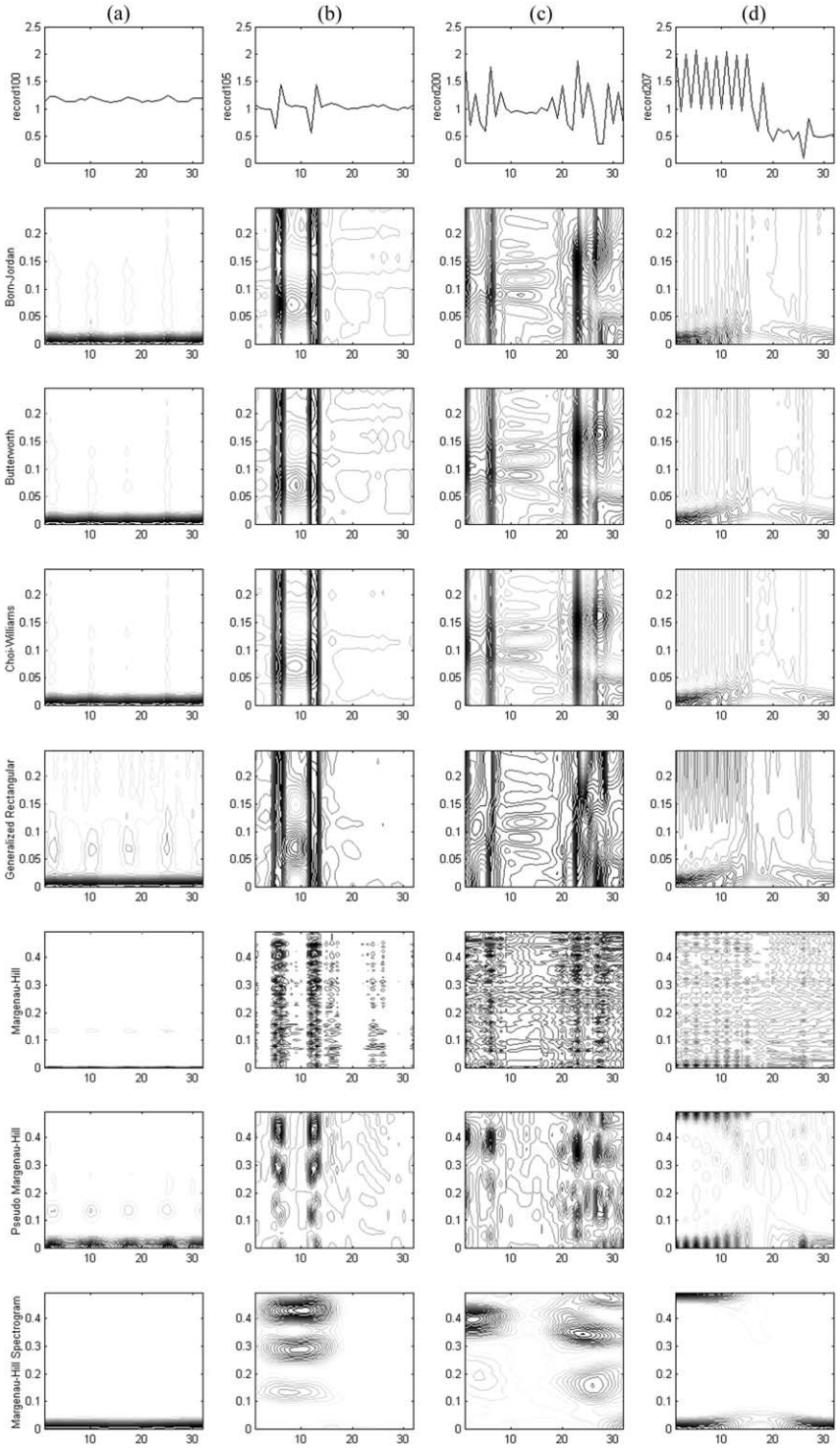

Fig. 1 PSD for RR-interval segments containing: (a) normal sinus rhythm (from recording 100 of the MIT-BIH database); (b) normal sinus rhythm with two premature ventricular contractions (from recording 105 of the MIT-BIH database); (c) normal sinus rhythm mixed with premature ventricular contractions (from recording 200 of the MIT-BIH database); (d) rhythm consisting of premature ventricular contractions, left bundle branch block and right bundle branch block beats changing to premature ventricular contractions and then to ventricular flutter/fibrillation (from recording 207 of the MIT-BIH database).

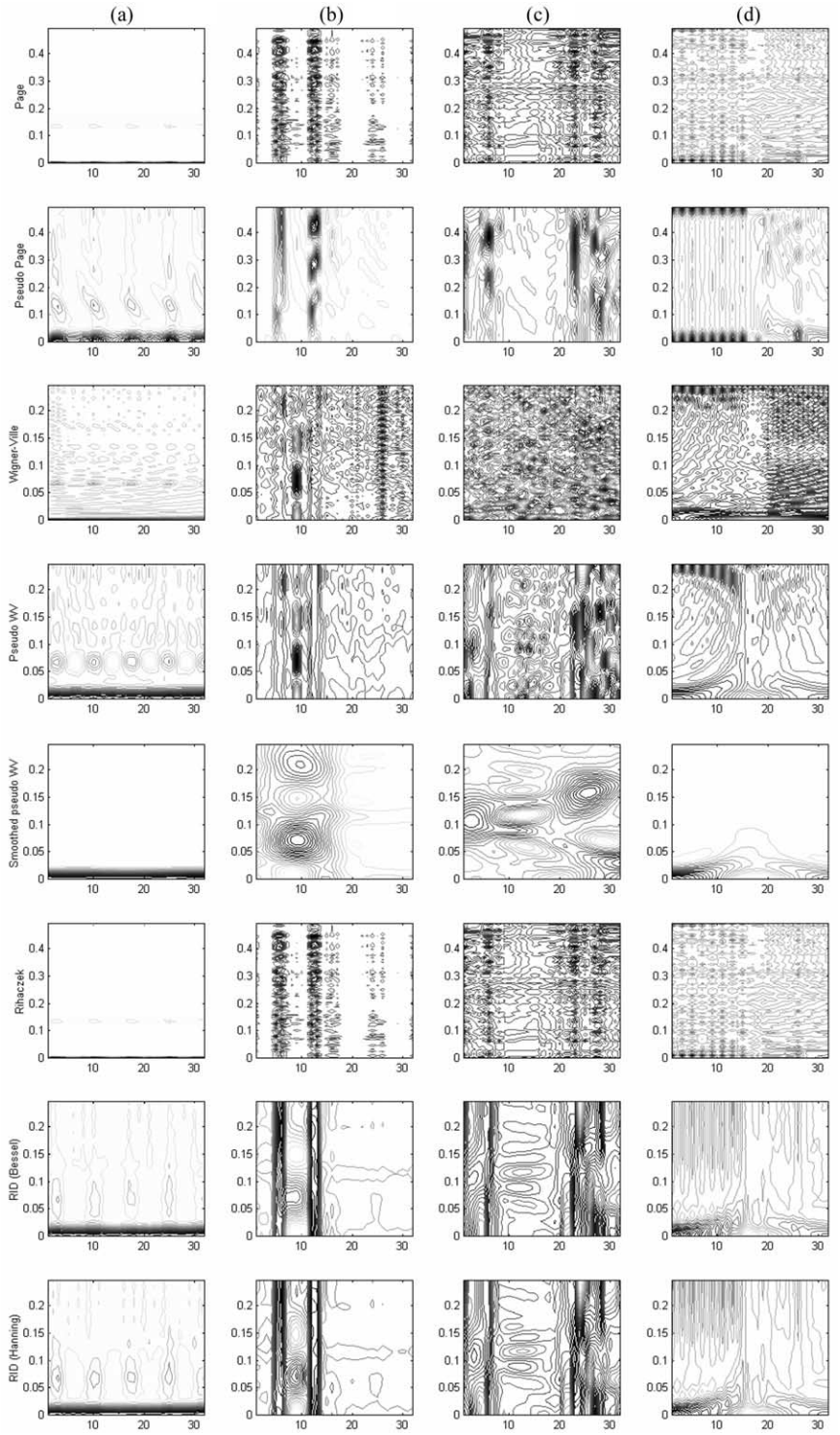

Fig. 1 (*Continued*).

For STFT and each TFD we train a feed-forward back-propagation neural network, using 1426 patterns randomly chosen from the total of 3426 patterns as training set. The architecture is similar to the one used in time domain analysis: six inputs, one hidden layer with 20 neurons and one output being a real number in the interval [0,1]. Finally, we result in a set with 19 neural networks (one for each method). The outputs of the neural networks are fed into a set of decision rules (forth stage), which is common for both procedures.

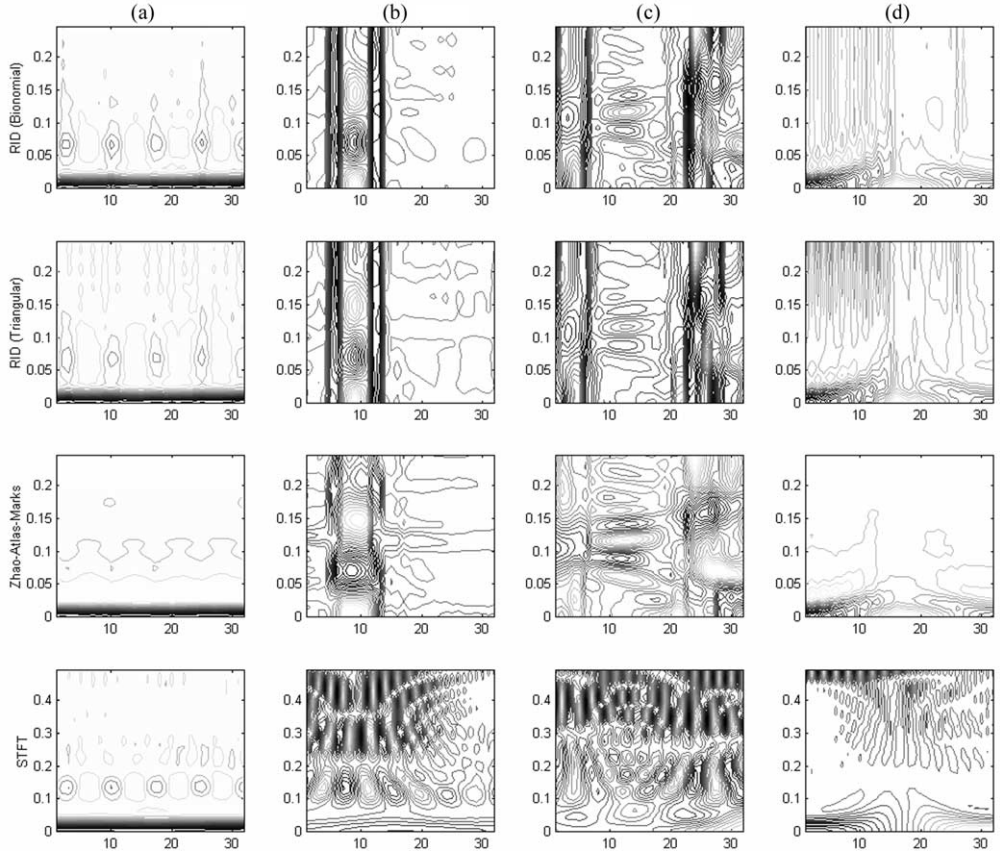

Fig. 1 (*Continued*).

2.4. Arrhythmia detection

For both time domain and $t-f$ analysis we use the remaining 2000 segments of the segmented dataset as test set. The outputs from all neural networks trained for each approach (63 for time domain analysis and 19 for $t-f$ analysis) are fed into the following decision rules to classify each segment as normal or arrhythmic:

- Average: For each segment we calculate the average of the outputs of all neural networks and a threshold 0.5 is used for the final decision, i.e.

$$T = \begin{cases} \text{Normal}(0) & \text{if } \dfrac{\sum_{i=1}^{N} y_i}{N} \leq 0.5 \\ \text{Arrhythmic}(1) & \text{if } \dfrac{\sum_{i=1}^{N} y_i}{N} > 0.5 \end{cases} \quad (3)$$

where T is the final decision; N, the number of the neural networks and y_i is the output of the ith neural network.

- Vote: For each segment all neural networks vote if it is arrhythmic, with threshold 0.5, i.e.:

$$A_i = \begin{cases} 0 & \text{if } y_i \leq 0.5 \\ 1 & \text{if } y_i > 0.5 \end{cases} \quad (4)$$

where y_i is the output of the ith neural network and A_i the vote of the ith neural network. If more than half votes are accumulated then the decision is ''Arrhythmic'', otherwise is ''Normal'', i.e.

$$T = \begin{cases} \text{Normal}(0) & \text{if } \sum_{i=1}^{N} A_i \leq \dfrac{N}{2} \\ \text{Arrhythmic}(1) & \text{if } \sum_{i=1}^{N} A_i > \dfrac{N}{2} \end{cases} \quad (5)$$

- Decision vote: Each neural network ''decides'' if it will vote using:

$$\Psi_i = \begin{cases} 0 & \text{if } |y_i - 0.5| \leq 0.1 \\ y_i & \text{if } |y_i - 0.5| > 0.1 \end{cases}, \quad (6)$$

where y_i is the output of the ith neural network and Ψ_i the vote of the ith neural network. If all neural networks vote 0 for a segment then the vote is calculated as:

$$\Psi_i = y_i \quad (7)$$

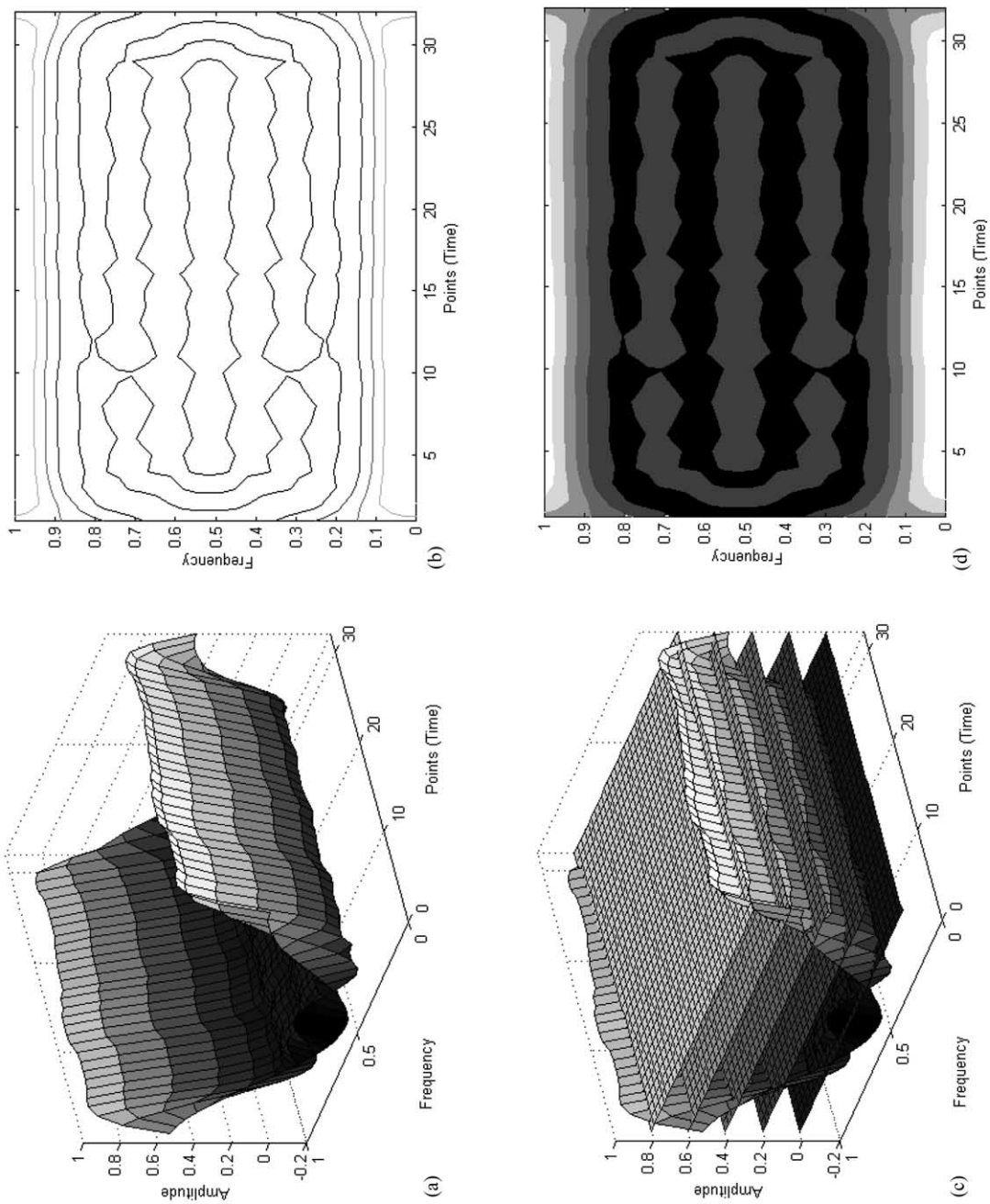

Fig. 2 (a) TFD, (b) horizontal slices, (c) traces, (d) features for $t-f$ methods.

Table 4 Results for sensitivity and specificity for neural networks

(*a*) *Trained with time features*

Combination	Sensitivity (%)	Specificity (%)	Combination	Sensitivity (%)	Specificity (%)
1	74	62	6	85	47
2	60	86	16	74	66
12	77	76	26	74	76
3	60	86	126	77	80
13	76	74	36	73	77
23	69	77	136	79	75
123	77	75	236	72	76
4	74	44	1236	80	77
14	72	65	46	81	49
24	69	76	146	74	65
124	74	75	246	75	75
34	62	84	1246	77	77
134	77	75	346	76	76
234	68	79	1346	79	77
1234	76	71	2346	73	75
5	83	40	12346	75	78
15	69	69	56	79	49
25	71	73	156	73	67
125	73	76	256	72	78
35	68	79	1256	75	79
135	75	77	356	76	73
235	69	81	1356	77	77
1235	79	76	2356	73	76
45	81	40	12356	78	78
145	69	67	456	76	53
245	70	72	1456	73	70
1245	75	74	2456	74	75
345	66	77	12456	80	72
1345	76	75	3456	77	72
2345	71	78	13456	73	77
12345	78	71	23456	75	74
			123456	78	72

(*b*) *Trained with t–f features*

Distribution	Sensitivity (%)	Specificity (%)
Born-Jordan	72	74
Butterworth	71	78
Choi-Williams	76	73
Generalized Rectangular	74	80
Margenau-Hill	73	76
Pseudo Margenau-Hill	74	76
Margenau-Hill Spectrogram	80	82
Page	74	84
Pseudo Page	80	84
Wigner-Ville	69	76
PWV	70	84
SPWV	75	82
Rihaczek	75	80
Reduced Interference (Bessel Window)	76	79
Reduced Interference (Hanning Window)	75	72
Reduced Interference (Binomial Window)	71	76
Reduced Interference (Triangular Window)	73	76
Zhao-Atlas-Marks	80	78
STFT	70	73

The average of all votes is used with threshold 0.5 for the final decision, i.e.

$$T = \begin{cases} \text{Normal}(0) & \text{if } \dfrac{\sum_{i=1}^{N} \Psi_i}{N} \leq 0.5 \\ \text{Arrhythmic}(1) & \text{if } \dfrac{\sum_{i=1}^{N} \Psi_i}{N} > 0.5 \end{cases} \quad (8)$$

The transfer function used among the layers is the hyperbolic tangent sigmoid function. The training function is the Levenberg–Marquardt back propagation method [55]. We use the mean squared error performance function, which measures the network's performance using the mean of squared errors.

2.5. Standard spectral analysis

Standard spectral analysis was applied to the RR-interval signal and used for arrhythmia detection and the results are compared with the proposed techniques. For each 32 RR-interval segment we apply Fourier analysis. We used principal component analysis (PCA) to reduce the number of Fourier coefficients. The minimum fraction variance for components was set to 3 and 4% that lead to the reduction of the number of coefficients from 32 to 16 and 5, respectively. A feed-forward back-propagation neural network was trained, using 1426 patterns randomly chosen from the total of 3426 patterns as training set. The architecture of the neural network is similar to the one used before for time domain and $t-f$ analysis: 16 inputs for the case of 3% minimum fraction variance for components in PCA and five inputs in the case of 4%, one hidden layer with 20 neurons and one output being a real number in the interval [0,1].

We have also applied autoregressive moving average (ARMA) analysis using Prony's and Steiglitz–McBride methods. The obtained parameters were used for the training of a feed-forward back-propagation neural network. 1426 patterns randomly chosen from the total of 3426 patterns were used as training set. The architecture of the neural networks is similar to the one used in time domain and $t-f$ analysis.

Table 5 Results for sensitivity and specificity using (a) time domain analysis combined with decision rules (b) $t-f$ analysis combined with decision rules (c) spectral analysis

Decision rule	Sensitivity (%)	Specificity (%)
(*a*) *Time domain analysis with decision rules*		
Average	80.68	78.18
Vote	82.60	78.43
Decision vote	87.53	89.48
(*b*) *t−f analysis with decision rules*		
Average	87.64	88.65
Vote	86.84	89.25
Decision vote	89.95	92.91
Method	Sensitivity (%)	Specificity (%)
(*c*) *Spectral analysis*		
DFT with PCA (3%)	73.14	71.55
DFT with PCA (4%)	74.74	71.02
Prony (6,4)	72.95	70.41
Steiglitz–McBride (2,8)	70.67	73.93

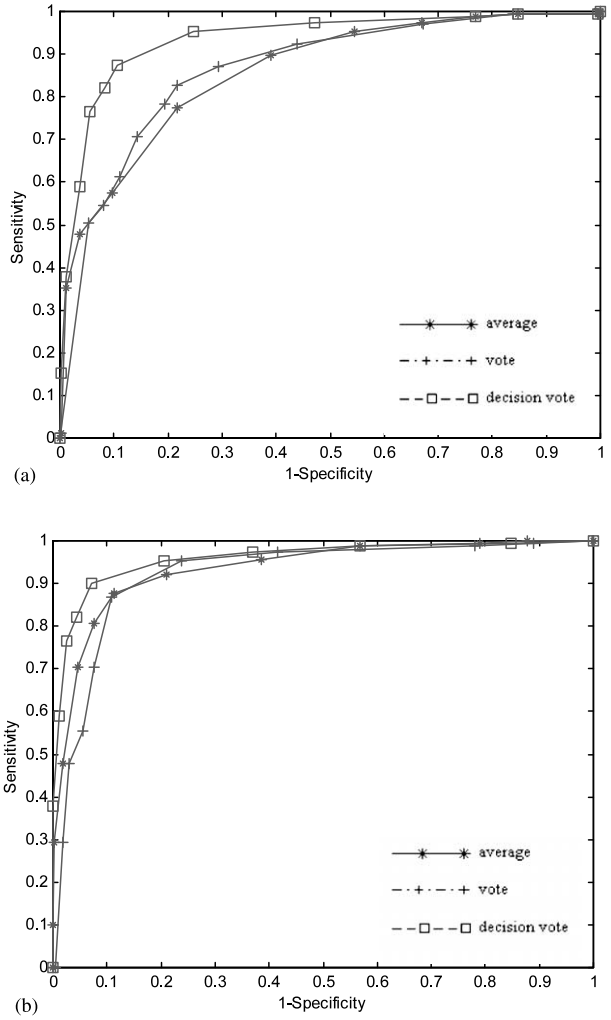

Fig. 3 (a) ROC curve for decision rules for neural networks trained with time features. (b) ROC curve for decision rules for neural networks trained with $t-f$ features.

Table 6 AUC marker results for decision rules

	AUC marker	
Decision rule	Time	$t-f$
Average	85.91%	93.53%
Vote	86.32%	92.27%
Weight vote	93.46%	95.83%

3. Results

The corresponding sensitivity and specificity for arrhythmic segment detection for each neural network are computed. The results for sensitivity and specificity, for the 63 neural networks trained with time feature combinations and the 19 neural networks trained with $t-f$ features, are reported in Table 4a and b, respectively. The results for a single neural network are not satisfactory (average sensitivity and specificity: 74 and 72% for neural networks trained with time features and 74 and 78% for neural networks trained with $t-f$ features). Therefore, a single neural network cannot be used for arrhythmia detection. However, we have observed the following:

1) Each neural network results in high sensitivity and specificity for signal segments for which the output is lower than 0.3 or higher than 0.7. This

Table 7 Comparative results with other studies in the literature

Author	Dataset	Arrhythmia types/Methods	Results	
			Sensitivity (%)	Specificity (%)
Thakor-Zhu Pan [4]	170 records (8 s)	Ventricular Fibrillation Ventricular Tachycardia		
Clayton-Muray	70 extracts (4 s)	Ventricular Fibrilation		
Campbell [6]		Threshold Crossing Intervals	46	72
		Autocorrelation Function	67	38
		VF Filter Leakage	77	55
		Signal Spectrum Shape	53	93
Thakor, Natarajah	ECGs from 30 patients	Supraventricular Tachycardia		
Tomaselli [5]		Ventricular Tachycardia		
Clayton-Muray	70 extracts (4 s)	Ventricular fibrilation		
Campbell [7]		Neural networks	84	59
Yang, Device, MacFariane [8]	2363 ECGs	Atrial fibrillation	92	93
Afonso-Tompkins [10]	Staley arrhythmia database	Ventricular fibrillation		
	MIT arrhythmia database			
Khadra,	45 ECGs	Ventricular fibrillation	91.7	83.3
AlFahoum	8 NR, 12 VF, 13 VT, 12 AF	Atrial Fibrillation	91.7	91.7
AlNashash [11]		Ventricular Tachycardia	84.6	92.3
		Normal Rhythm	87.5	87.5
AlFahoum-Howitt [12]	158 ECGs	Ventricular Fibrillation	100	100
	(37 NR, 49 VF, 49 VT, 20 AF)	Atrial Fibrillation	95.2	85.7
		Ventricular Tachycardia	100	100
		Normal Rhythm	92.5	97.5
Minami	700 QRS	Ventricular Fibrillation	92	92
Nakajima	(150 VT, 250 VF, 300 NR)	Ventricular Tachycardia	80	96
Toyashima [9]		Normal Rhythm	99	98
Zhang-Zhu	170 records (48 s)		100% identification after 7 s	
Thakor-Wang [13]	85 VT, 85 VF, 34 NR			
Wang-Zhu	180 records (6 s)	Ventricular Fibrillation	98.3	96.7
Thakor-Xu [14]	(60 VF, 60 AF, 60 VT)	Ventricular Tachycardia	95	99.2
		Atrial Fibrillation	98.3	100
This work	MIT arrhythmia database	All types included in MIT database	87.53	89.48
	48 ECGs 30 min length	Time analysis, t-f analysis	89.95	92.91

is because the output of the neural network can be viewed as a possibility function that decides if a segment is normal (result 0) or arrhythmic (result 1).

2) Each neural network results in low sensitivity and specificity for signal segments for which the output was close to 0.5 (i.e. in the interval $[0.5-k,\ 0.5+k]$ with $k \leq 0.2$). This is an uncertainty interval with high error rate.
3) For all signal segments there is a number of neural networks that can detect them correctly with output outside the uncertainty interval [0.45, 0.55] (i.e. $k=0.05$). When the uncertainty interval is larger (i.e. $k=0.1$, 0.15 or 0.2) the number of neural networks, which detect the same number of segments correctly, is reduced and for some segments there are no neural networks with output outside the uncertainty interval. We have used various uncertainty intervals and the best choice is [0.4, 0.6] (i.e. $k=0.1$).

The above observations lead us to the use of multiple identifiers combined with decision rules. The results for sensitivity and specificity when we use the decision rules on the neural networks' outputs are presented in Table 5. In Table 5 we present also the results for standard spectral analysis using Fourier analysis and parametric modeling with Prony's method, with numerator order 2 and denominator order 8, and Steiglitz–McBride method, with numerator order 6 and denominator order 4. For each decision rule the receiver operating characteristic (ROC) curve is computed. The ROC curves are shown in Fig. 3. Using the ROC curves the area under curve (AUC) marker is calculated and the results are presented in Table 6.

4. Discussion—conclusions

We have developed an automatic procedure for the detection of arrhythmias using heart rate features. The outcome of the method is the classification of the ECG signal segments as ''normal'' or ''arrhythmic''. The method is based on time analysis and $t-f$ analysis features. If time features are chosen their combination lead us to 63 neural networks. If $t-f$ analysis is followed then we result into 19 neural networks. We have proven that a single neural network does not offer satisfactory results in terms of sensitivity and specificity for arrhythmia detection and this imposed the use of decision rules, which combine the outputs of all neural networks. One of the advantages of the method is that the single use of heart rate features can lead to the identification of arrhythmic intervals in ECG recordings. This does not depend on the type of arrhythmia.

For the time domain approach the average and vote decision rules result in low performance for both sensitivity and specificity (81 and 78%, respectively). This is expected since in both cases the neural networks' outputs inside the uncertainty interval have high error rate. The sensitivity and specificity for decision vote are 87.5 and 89.5%, respectively. Average and vote decision rules for the $t-f$ features resulted in 87% sensitivity and 89% specificity. The decision vote results superior (90% sensitivity and 93% sensitivity). The obtained sensitivity and specificity for using Fourier analysis followed by PCA are 73.14 and 71.55% for minimum fraction variance 3, 74.74 and 71.02% for minimum fraction variance 4%, respectively. Parametric modeling resulted in 72.95% for sensitivity and 70.41% for specificity using Prony's method and 70.67% for sensitivity and 73.93% for specificity using Steiglitz–McBride method.

Several researchers have addressed the problem of arrhythmia detection using ECG features and heart rate analysis. A summary of those studies with the results obtained in terms of sensitivity and specificity is provided in Table 7. Most of the authors [4–14] focus their work on the detection of some particular types of arrhythmia (ventricular fibrillation, atrial fibrillation, ventricular tachycardia, supraventricular tachycardia). Our method compares well since it addresses the arrhythmia detection for all types of arrhythmia, using only heart rate features. A drawback is that some arrhythmia types (such as left bundle branch block and right bundle branch block beats) cannot be detected using only heart rate features. Another important feature is that some of the methods use a specific dataset so as to be evaluated, therefore, a direct comparison with our method is not a simple task. The dataset used for each method is given in Table 7. In our case we have used all the recordings of the ''standard'' MIT-BIH arrhythmia database to evaluate the proposed method.

Our study is based on the analysis of the RR-interval duration so the proposed method is capable of detecting arrhythmia types that produce irregularities on the RR intervals, the HRV or the heart rhythm. Left bundle branch block and right bundle branch block beats do not produce such artifacts, therefore, they cannot be detected using only heart rate features. Instead of excluding these beats from the analysis we classify them as ''normal'' because we wanted the method to be as general as possible. Probably this ''misclassification'' affects the results but no tests

were made on this matter so we cannot make any comments on this subject.

Besides the QRS detection and the extraction of the RR-interval duration signal, there is no other processing of the ECG recording in our study, such as P wave or T wave detection which will make the process more complicated and time consuming. Therefore, noisy data can be analyzed because QRS detection algorithms perform well. The exclusive use of the RR-interval duration signal leads to a high reduction of input and processing data, compared with other ECG analysis methods. Moreover, the final decision is not based on a single identifier but on the combined results of a set of identifiers. Therefore, the system is expected to have high generalization capability. Due to the short processing time and the generalization capability of the method we believe that the proposed approach can be used in real time arrhythmia detection systems. In addition, RR-interval duration features can be used for the classification of detected arrhythmic segments into several arrhythmia types.

Acknowledgements

The authors are grateful to Professor D. Sideris, Professor A. Likas and Professor N. Galatsanos for useful comments and suggestions.

References

[1] E. Sandoe, B. Sigurd, Arrhythmia—a Guide to Clinical Electrocardiology, Verlags GmbH, Bingen, 1991 (Chapter 3).
[2] L. Goldberger, E. Goldberger, Clinical Electrocardiography, The Mosby Company, Saint Louis, 1977 (Chapter 11).
[3] D.A. Sideris, Primary Cardiology, Grigorios K. Parisianos, Athens, 1991 Scientific Editions, in Greek.
[4] N.V. Thakor, Y.S. Zhu, K.Y. Pan, Ventricular tachycardia and fibrillation detection be a sequential hypothesis testing algorithm, IEEE Trans. Biomed. Eng. 37 (9) (1990) 837—843.
[5] N.V. Thakor, A. Natarajan, G. Tomaselli, Multiway sequential hypothesis testing for tachyarrhythmia discrimination, IEEE Trans. Biomed. Eng. 41 (5) (1994) 480—487.
[6] R.H. Clayton, A. Murray, R.W.F. Campbell, Comparison of four techniques for recognition of ventricular fibrillation of the surface ECG, Med. Biol. Eng. Comp. 31 (1993) 111—117.
[7] R.H. Clayton, A. Murray, R.W.F. Campbell, Recognition of ventricular fibrillation using neural networks, Med. Biol. Eng. Comp. 32 (1994) 217—220.
[8] T.F. Yang, B. Device, P.W. Macfarlane, Artificial neural networks for the diagnosis of atrial fibrillation, Med. Biol. Eng. Comput. 32 (1994) 615—619.
[9] K. Minami, H. Nakajima, T. Toyoshima, Real-time discrimination of ventricular tachyarrhythmia with Fourier-transform neural network, IEEE Trans. Biomed. Eng. 46 (2) (1999) 179—185.
[10] V.X. Afonso, W.J. Tompkins, Detecting ventricular fibrillation, IEEE Eng. Med. Biol. 14 (1995) 152—159.
[11] L. Khadra, A.S. Al-Fahoum, H. Al-Nashash, Detection of life-threatening cardiac arrhythmias using wavelet transformation, Med. Biol. Eng. Comput. 35 (1997) 626—632.
[12] A.S. Al-Fahoum, I. Howitt, Combined wavelet transformation and radial basis neural networks for classifying life-threatening cardiac arrhythmias, Med. Biol. Eng. Comput. 37 (1999) 566—573.
[13] X.S. Zhang, Y.S. Zhu, N.V. Thakor, Z.Z. Wang, Detecting ventricular tachycardia and fibrillation by complexity measure, IEEE Trans. Biomed. Eng. 46 (5) (1999) 548—555.
[14] Y. Wang, Y.S. Zhu, N.V. Thakor, Y.H. Xu, A short-time multifractal approach for arrhythmia detection based on fuzzy neural network, IEEE Trans. Biomed. Eng. 48 (9) (2001) 989—995.
[15] Task force of The European Society of Cardiology and The North American Society of Pacing and Electrophysiology, Heart rate variability: standards of measurement, physiological interpretation and clinical use, Eur. Heart J. 17 (1996) 354—381.
[16] R. Kleiger, P. Stein, M. Bosner, J. Rottman, Time domain measurement of heart rate variability, Cardiol. Clin. 10 (1992) 487—498.
[17] R.E. Kleiger, P.K. Stein, M.S. Bosner, J.N. Rottman, Time-domain measurements of heart rate variability, in: M. Malik, A.J. Camm (Eds.), Heart Rate Variability, Futura Publishing Company, Armonk, NY, 1995 (Chapter 3).
[18] M. Malik, Geometrical methods for heart rate variability assessment, in: M. Malik, A.J. Camm (Eds.), Heart Rate Variability, Futura Publishing Company, Armonk, NY, 1995 (Chapter 4).
[19] F. Azuaje, W. Dubitzky, P. Lopes, N. Black, K. Adamson, X. Wu, J.A. White, Predicting coronary disease risk based on short-term RR-interval measurements: a neural network approach, Artif. Intell. Med. 15 (3) (1999) 275—297.
[20] S. Cerutti, A.M. Bianchi, L.T. Mainardi, Spectral analysis of heart rate variability signal, in: M. Malik, A.J. Camm (Eds.), Heart Rate Variability, Futura Publishing Company, Armonk, NY, 1995 (Chapter 5).
[21] C. Albrecht, Estimation of heart rate power spectrum bands from real world data: dealing with ectopic beats with noisy data, Comp. Cardiol. 15 (1998) 311—314.
[22] A. Malliani, M. Pagani, F. Lombardi, S. Cerrutti, Cardiovascular neural regulation explored in the frequency domain, Circulation 84 (2) (1991) 482—492.
[23] J.T. Bigger, J.L. Fleiss, R.C. Steinman, L.M. Rolnitzky, R.E. Kleiger, J.N. Rottman, Frequency domain measures of heart period variability and mortality after myocardial infarction, Circulation 85 (1) (1992) 164—171.
[24] A.M. Bianchi, L.T. Mainardi, E. Petrucci, M.G. Signorini, M. Mainardi, S. Cerutti, Time-variant power spectrum analysis for the detection of transient episodes in HRV signal, IEEE Trans. Biomed. Eng. 40 (1993) 136—144.
[25] L. Basano, F. Canepa, P. Ottonello, Real time spectral analysis of HRV signals: an interactive and user-friendly PC system, Comput. Methods Programs Biomed. 55 (1) (1998) 69—76.
[26] G. Schmidt, G.E. Morfil, Nonlinear analysis of heart rate variability assesment, in: M. Malik, A.J. Camm (Eds.), Heart Rate Variability, Futura Publishing Company, Armonk, NY, 1995 (Chapter 7).
[27] T. Mekikallio, Analysis of Heart Rate Dynamics by Methods Derived from Nonlinear Mathematics, Oulu University Library, Oulu, 1999 (Chapter 2).
[28] V. Novak, P. Novak, J. de Champlain, A.R. Le Blanc, R. Martin, R. Nadeau, Influence of respiration on heart rate and blood pressure fluctuations, J. Appl. Physiol. 74 (2) (1993) 617—626.

[29] P. Novak, V. Novak, Time/frequency mapping of the heart rate, blood pressure and respiratory signals, Med. Biol. Eng. Comput. 31 (2) (1993) 103—110.
[30] V. Novak, P. Novak, M. deMarchie, R. Schondorf, The effect of severe brain stem injury on heart rate and blood pressure oscillation, Clin. Auton. Res. 5 (1) (1995) 24—30.
[31] V. Novak, P. Novak, T.L. Opfer-Gehrking, P.A. Low, Postural tachycardia syndrome: time frequency mapping, J. Auton. Nerv. Syst. 61 (3) (1996) 313—320.
[32] A. Bharucha, V. Novak, M. Camilleri, A.Z. Zinsmeister, R.B. Hanson, P.A. Low, a^2-Adrenergic modulation of colonic tone during hyperventilation, Am. J. Physiol. 61 (1997) 273 (Gastrointest Liver Physiol 36): G1135—G1140.
[33] V. Novak, A.L. Reeves, P. Novak, P.A. Low, F.W. Sharbrough, Time—frequency mapping of R—R interval during complex partial seizures of temporal lobe origin, J. Auton. Nerv. Syst. 77 (2—3) (1999) 195—202.
[34] H.H. Huang, H.L. Chan, P.L. Lin, C.P. Wu, C.H. Huang, Time—frequency spectral analysis of heart rate variability during induction of general anaesthesia, Br. J. Anaesth. 79 (6) (1997) 754—758.
[35] H.L. Chan, J.L. Lin, C.C. Du, C.P. Wu, Time—frequency distribution of heart rate variability below 0.05 Hz by Wigner-Ville spectral analysis in congestive heart failure patients, Med. Eng. Phys. 19 (6) (1997) 581—587.
[36] H.L. Chan, J.L. Lin, H.H. Huang, C.P. Wu, Elimination of interference component in Wigner-Ville distribution for the signal with 1/f spectral characteristic, IEEE Trans. Biomed. Eng. 44 (9) (1997) 903—907.
[37] S. Akselrod, D. Gordon, F.A. Ubel, D.C. Shannon, A.C. Barger, R.J. Cohen, Power spectrum analysis of heart rate fluctuation: a quantitative probe of beat to beat cardiovascular control, Science 213 (1981) 220—222.
[38] L. Keselbrener, A. Baharav, S. Akselrod, Estimation of fast vagal response by time-dependent analysis of heart rate variability in normal subjects, Clin. Auton. Res. 6 (6) (1996) 321—327.
[39] L. Keselbrener, S. Akselrod, Selective discrete Fourier transform algorithm for time—frequency analysis: method and application on simulated and cardiovascular signals, IEEE Trans. Biomed. Eng. 43 (8) (1996) 789—802.
[40] L. Keselbrener, S. Akselrod, Time—frequency analysis of transient signals-application to cardiovascular control, Physica A 249 (1—4) (1998) 482—490.
[41] F. Claria, M. Vallverdu, R. Baranowski, L. Chojnowska, P. Caminal, Time—frequency analysis of the RT and RR variability to stratify hypertrophic cardiomyopathy patients, Comput. Biomed. Res. 33 (4) (2000) 416—430.
[42] H.G. Steenis, J.H.M. Tulen, The exponential distribution applied to nonequidistandly sampled cardiovascular time series, Comput. Biomed. Res. 29 (1996) 174—193.
[43] S. Stamatelopoulos, D. Sideris, L. Anthopoulos, S. Moulopoulos, Observations for a new study method for characteristics of cardiac disease, Proc. Athens Med. Soc. C′ (1970) 284—296 in Greek.
[44] MIT-BIH Arrhythmia Database CD-ROM, 3rd ed., Harvard-MIT Division of Health Sciences and Technology, 1997.
[45] G.B. Moody, R.G. Mark, The impact of the MIT-BIH arrhythmia database, Comput. Biomed. Res. 29 (1996) 174—193.
[46] L. Cohen, Time—frequency distributions—a review, Proc. IEEE 77 (7) (1989) 941—981.
[47] F. Auger, P. Flandrin, P. Goncalves, O. Lemoine, Time—Frequency Toolbox Tutorial, CNRS, RICE University, France, USA, 1995—1996.
[48] F. Auger, P. Flandrin, P. Goncalves, O. Lemoine, Time—Frequency Toolbox Reference Guide, CNRS, RICE University, France, USA, 1995—1996.
[49] A. Papandreou, G.F. Bourdreaux-Bartels, Generalization of the Choi-Williams distribution and the Butterworth distribution for time—frequency analysis, IEEE Trans. Sig. Proc. 41 (1) (1993) 463—472.
[50] L. Cohen, Introduction: a primer on time—frequency analysis, in: B. Boashash (Ed.), Time—Frequency Signal Analysis, Wiley, , 1992 (Chapter 1).
[51] B. Boashash, G. Jones, Instantaneous frequency and time—frequency distributions, in: B. Boashash (Ed.), Time—Frequency Signal Analysis, Wiley, B. Boashash, 1992 (Chapter 2).
[52] W.J. Williams, J. Jeong, Reduced interference time—frequency distributions, in: B. Boashash (Ed.), Time—Frequency Signal Analysis, Wiley, , 1992 (Chapter 3).
[53] W.J. Williams, Recent advances in time—frequency representations: some theoretical foundation, in: M. Akay (Ed.), Time Frequency and Wavelets in Biomedical Signal Processing, IEEE Press, New York, 1998 (Chapter 1).
[54] W.J. Williams, Biological applications and interpretations of time—frequency signal analysis, in: M. Akay (Ed.), Time Frequency and Wavelets in Biomedical Signal Processing, IEEE Press, New York, 1998 (Chapter 2).
[55] Neural Network Toolbox, ver 3.0, Mathworks Inc., 1992—1997.